JOURNAL OF MATERIALS SCIENCE **36** (2001) 285–295

Review
Durability of materials in molten aluminum alloys

M. YAN
Department of Materials Science and Engineering, Zhejiang University, Hangzhou 310027, People's Republic of China
E-mail: mse_yanmi@dial.zju.edu.cn

Z. FAN
Department of Materials Engineering, Brunel University, Uxbridge, Middlesex, UB8 3PH, UK

The durability of metals and ceramics in molten aluminum is a great concern in engineering applications such as die casting, containment of liquid metals and semi-solid processing. This paper summarizes related work along with the experimental results from our laboratory. Most of the important engineering materials are included. Ceramics such as graphite, aluminosilicate refractories, AlN, Al_2O_3, Si_3N_4, sialons are characterized as inert in molten aluminum and its alloys. The corrosion resistance of metals is generally poorer than that of inert ceramics, although the durability of titanium and niobium is relatively good. Factors affecting the material durability in molten aluminum, including the interfacial layers, dynamic agitation, surface coatings and grain size are also discussed.

1. Introduction

The durability of materials, including both metals and ceramics, exposed to molten aluminum is an important consideration in many engineering applications since molten aluminum is one of the most aggressive metals to a number of materials. Important examples are die casting, containment of liquid aluminum and semi-solid processing. Molten aluminum can cause considerable corrosion of the handling and container materials, leading to an insufficient and, above all, unpredictable lifetime. In the aluminum industry, refractory performance against corrosion is an important factor affecting the quality of metal produced and the durability of furnace lining [1–3]. The tolerance of aluminum alloy castings may be affected by the wear of dies caused by aluminum flow [4, 5]. The search for materials compatible with molten aluminum is of great importance in the service environment of semi-solid processing of aluminum, where components are subject to complex stress conditions [6, 7]. Under such complex stress conditions materials should possess not only enough erosion resistance, but also high fatigue resistance, satisfactory creep strength and toughness. Consequently, those materials usually used for containment of molten aluminum, such as graphite and aluminosilicate refractories, cannot be utilized, and few materials have been characterized as qualified.

Chemical corrosion and physical erosion are the main mechanisms of materials failure in molten aluminum. Chemical corrosion refers to penetration and dissolution of materials by the melt as well as the formation of interphase layers, prevailing when relative motion between the solid materials and the melt is negligible [8]. Erosion is dominant when there is a swift flow of melt relative to the surface of the solid, and becomes more severe when there are hard particles in the melt, where mechanical wear occurs on the materials surface. At present, there have been no comprehensive reports on the performance of materials against aluminum attack.

The selection of materials with suitable durability in molten aluminum requires an understanding not only on the thermodynamic principles governing the chemical interaction, but also on the mechanisms and kinetics of the reaction process. However, the experimental data associated with engineering metals or ceramics subjected to molten metal corrosion/erosion are limited. The insufficient information may be compensated to some extent from the work on other related studies, such as the wetting behavior of liquid aluminum, the joining of aluminum with other materials and the fabrication of Al-matrix composites. In such cases the interfacial reaction or compatibility of ceramic and metallic materials with molten aluminum is also of great concern. The sessile drop method is usually used to investigate wetting behavior. In this technique the contact angle between a droplet and the substrate is measured, and any interfacial reaction is normally examined through sectioning the interfaces [9–13]. In the fabrication of aluminum matrix composites, the infiltration of the reinforcement network by molten aluminum and the homogeneity of the matrix are partially governed by wetting of the reinforcement by aluminum and the chemical interaction between the reinforcement and aluminum matrix [14–17]. In joining processes the

compounds formed and the interface microstructures with aluminum alloys have a great influence on joint reliability [18]. Although these investigations focus on their own predetermined objectives, and the results obtained regarding material reactivities with liquid aluminum may not be directly converted to corrosion rates, they are useful indicators of the durability of various materials in liquid aluminum and its alloys, particularly in aspects such as thermodynamic analyses and mechanisms of chemical reactions.

This paper summarizes the available literature, augmented by recent experimental results in our laboratory. Primary attention is paid to the important engineering materials and those supposed to be inert in molten aluminum.

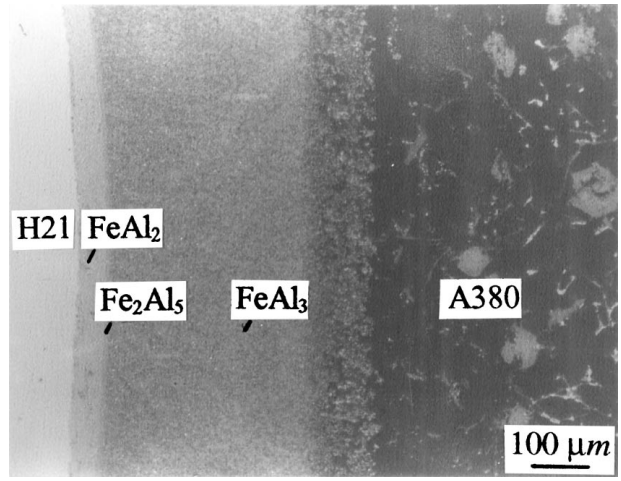

Figure 1 Interfacial morphology of H21 steel sample in molten A380 alloy. Rotating at 700°C with a speed of 300 rpm [27].

2. Metallic alloys

In selection of metals applied in molten aluminum, the respective binary phase diagrams of elements, particularly the solubility of elements in molten aluminum, and their melting temperatures are important indicators. The formation of peritectics implies an increase in the free energy with dissolution. It is beneficial for peritectics formers, including Ti, Nb, W, V and Zr, to resist dissolution by molten aluminum. On the contrary, when eutectics formers like Fe, Ni, Co and Cu are dissolved in molten aluminum, the free energy of melt will decrease, raising up the dissolution tendency.

Interactions of metallic materials with molten aluminum possess some common features. They all form intermediate layers of intermetallic compounds between the metal substrates and molten aluminum. These layers usually consist of either one phase, or several phases, depending on the composition of the substrate and the reaction conditions. If different phases are formed the zone consists of successive layers of intermetallic compounds. The layer adjacent the substrate contains the highest content of the base element of the substrate, while the layer next to molten aluminum is always aluminum-rich. However, the corrosion or erosion rate in molten aluminum varies from metal to metal. Major metallic materials investigated are ferrous, nickel and titanium alloys, which are discussed separately in this section.

2.1. Ferrous alloys

Most of the dies for production of aluminum components in the casting industry are made of ferrous alloys. Reports on the corrosion/erosion rates of metals in liquid aluminum mainly focus on ferrous alloys, especially on various steels. A intermediate zone (up to hundreds of microns thick) forms between the metal substrate and molten aluminum [4, 5, 19–33]. The intermediate zone consists of successive layers of iron aluminates. Usually two intermetallic layers, namely, θ-$FeAl_3$ directly adjacent the aluminum alloy and η-Fe_2Al_5 adjacent the steel substrate, form at the interface [21–26]. ζ-$FeAl_2$ is also observed for H13 and H21 tool steels submerged in liquid A380 alloy between the steel and η-Fe_2Al_5 phase (Fig. 1) [5, 27]. Other iron-rich compounds present in the Al-Fe equilibrium diagram are never found in the intermediate zone. The formation of aluminum-rich Al-Fe compounds is related to the greater interdiffusion coefficients of aluminum in these compounds than in iron-rich Al-Fe compounds [28].

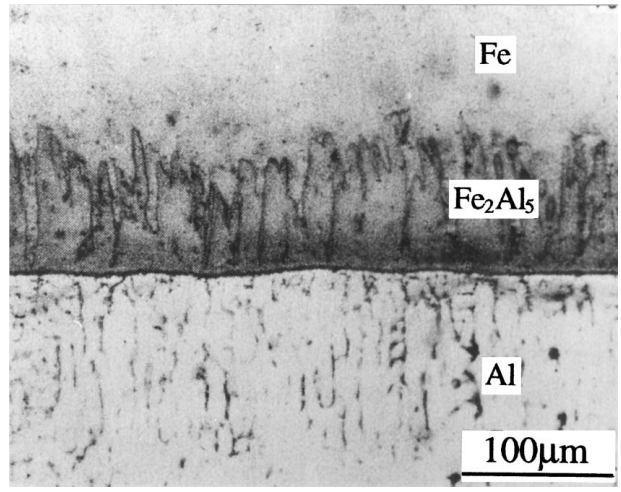

Figure 2 Micrograph of the interface of pure iron disc in pure aluminum. Rotating at 24.0 rad s^{-1} for 250 s at 700°C [20].

Various morphologies of the intermetallic compounds have been reported. In the case of pure solid iron and liquid aluminum, the Fe_2Al_5 layer grows irregularly into the iron substrate, forming a tongue-like morphology, as shown in Fig. 2 [20]. The growth direction of the Fe_2Al_5 phase is believed to coincide with the c axis of the orthorhombic unit cell, which causes the tongue-like morphology [24]. The $FeAl_3$ layer is compact, forming neighboring the liquid aluminum [21]. Although there have not been any data on its thickness, this layer is thin and sometimes cannot be observed. In the cases of alloy steels and molten aluminum alloys, the morphology varies and porosity is sometimes observed in the intermetallic layers [21–35]. The different morphologies and intermetallic layer thicknesses are believed to be associated with alloy additions and melt agitation.

TABLE I Comparison of microhardness of intermetallic compounds

Layer	Microhardness (HV, GPa) [30]	Layer	Microhardness (HV, kg/mm^2) [5]	Layer	Microhardness (HV, kg/mm^2) [27]
18Cr-10Ni stainless steel (in pure Al)	1.8 ± 0.2	H13 tool steel (in A380)	239	H21 tool steel (in A380)	271
		$FeAl_2$-type	985	$FeAl_2$-type	974
Fe_2Al_5-type	8.9 ± 0.9	Fe_2Al_5-type		Fe_2Al_5-type	
$FeAl_3$-type	4.5 to 3.06	$FeAl_3$-type	1096	$FeAl_3$-type	403
pure Al	0.6 ± 0.1	A380 alloy	100	A380 alloy	94

*: 1 GPa $\approx$ 100 kg/mm^2.

Fe-Al intermetallic compounds have well-defined crystal structures, and can exist in an extended composition range when alloying elements are contained in the steel. Alloying elements such as Cr, Ni may partly replace the iron atoms but do not change the compound crystal structure in the composition range of alloy steels. The dissolution of steel in liquid aluminum is non-selective and diffusion controlled after the initial reaction stage [30]. Alloy additions such as Si, Cr, Ni, Mn and Cu present in the intermediate zone, and reduce the intermetallic layer thickness. Among them Si is regarded as the most effective element [19, 21, 22, 34, 35]. Silicon atoms are assumed to occupy the structural vacancies of the Fe_2Al_5 phase [22, 31, 33], and Al-Fe-Si compounds are also observed to form in the intermediate zone, although their crystal structures are not always identified [4, 20, 22, 35]. Lamellar graphite in grey cast iron is found to reduce the intermetallic layer thickness more effectively than cementite in low carbon steel because graphite forms a diffusional barrier [36].

Protuberances are often observed to form at the outer layers of the reaction zones of ferrous samples [5, 21, 23], resulted from the dendritic growth of the iron aluminate. The protuberances are cylindrical at the base and topped by a cone, growing from the intermediate zone into the aluminum melt. The length of the protuberances can be as long as several tens of microns, up to over 100 microns. The continuously formed protuberances may not only increase the surface available for corrosion, but also break off at the bases into molten aluminum, leading to the loss of material both at the atomic scale and in blocks. Thus the presence of protuberances aggravates the loss of steels. When there exists rapid relative motion between the steel and liquid aluminum, protuberances are broken off from the substrate by the shear stress, and the interface of intermediate zone with aluminum are found to be planar [27, 30].

Intermetallic layers are significantly harder than the steel substrate. A comparison of typical microhardness values of intermetallic layers is given in Table I. The hardness of the intermediate zone is reduced significantly if there is porosity in it. This explains why the hardness of $FeAl_3$-type layers is much higher in Ref. [5], while drastically lower in Refs. [27] and [30]. The high hardness of interfacial layers is beneficial to wear resistance. However, the intermetallic layers on ferrous alloys do not provide good protection for the substrate. Due to the dissolution of iron and loss of interfacial compounds, the erosion rates of ferrous alloys in liquid aluminum alloys are usually high. The attack is further intensified when any relative motion exists between the solid ferrous alloy and molten aluminum. The loss rates of tool steels are demonstrated in Figs 3 and 4 as a function of the square root of test time [21, 27].

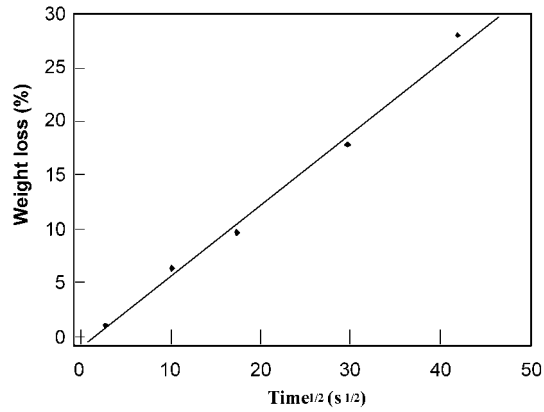

Figure 3 Weight loss of a tool steel immersed in pure aluminum at 800°C [21].

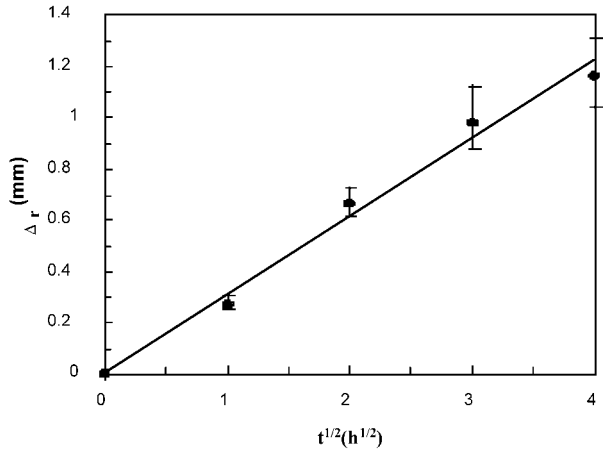

Figure 4 The radius decrease of rod-shaped H21 samples, Δr, vs. the square root of test time. Original sample diameter 10 mm, rotating in molten A380 alloy at 700°C with a speed of 300 rpm [27].

2.2. Nickel-base alloys

Nickel has been characterized as active with both liquid and solid aluminum [37–43]. The radius decrease rates

TABLE II Solubility of elements in pure liquid aluminum [44]

Temperature (°C)	Fe (%)	Cr (%)	Ni (%)	Ti (%)
700	3.2	0.7	9.0	0.2
750	4.9	1.3	13.2	0.3
800	6.8	2.4	17.3	0.5
850	7.9	4.2	26.2	0.7

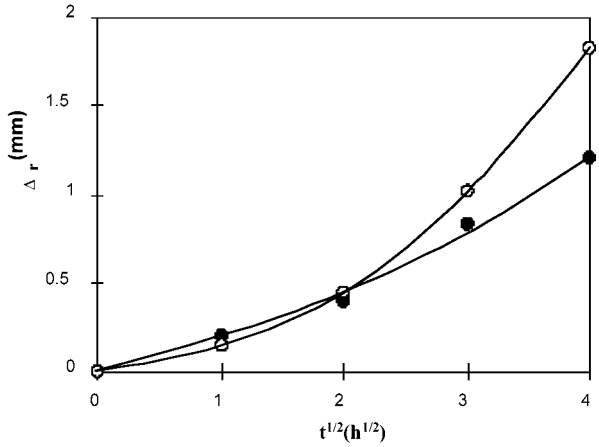

Figure 5 The radius decrease of Inconel 718 samples, Δr, vs. the square root of test time. Rotating in molten A380 alloy at 700°C with a speed of 300 rpm. ●: original sample diameter 16 mm, ○: original sample diameter 10 mm [37].

of Inconel 718 rods rotating in molten A380 aluminum alloy at 700°C are shown in Fig. 5 [37]. The high loss rates of nickel-base alloys are primarily due to the high solubility of nickel in liquid aluminum. The solubility of nickel at different temperatures is given in Table II, compared with that of other metallic elements [44]. Moreover, penetration of molten aluminum into the depth of nickel-base alloys can cause the alloy loss in blocks [37].

In the Ni-Al equilibrium phase diagram, four intermetallic phases, ϵ-Ni_3Al, δ-NiAl, γ-Ni_2Al_3, β-$NiAl_3$, and solid solution of nickel in aluminum form below 855°C. $NiAl_3$ and Ni_2Al_3 are found to be the only intermetallic phases in Al/Ni diffusion couples annealed at 610°C up to 66 hours [38]. After annealing as long as 340 h at 600°C Ni_3Al and NiAl are also found, in addition to Ni_2Al_3 and $NiAl_3$ [39, 40]. Solid nickel-liquid aluminum diffusion couples conducted at 700 and 750°C by Tsao *et al*. [41] also find two phases between the nickel plate and the molten aluminum (Fig. 6). They are Ni_2Al_3 adjacent the nickel plate, and $NiAl_3$ adjacent the molten aluminum. When solid nickel-base rod rotates relative to the aluminum melt, the $NiAl_3$-type layer continuously breaks off from the alloy surface, forming a laminar $NiAl_3$/Al intermediate zone (Fig. 7) [37].

The high reactivity of nickel with molten aluminum is used in the production of alumina-reinforced aluminum matrix composites. Nickel plating of the alumina phase overcomes the non-wetting [42, 43]. In stainless steel, nickel preferentially dissolves in liquid aluminum from the intermediate zone [30].

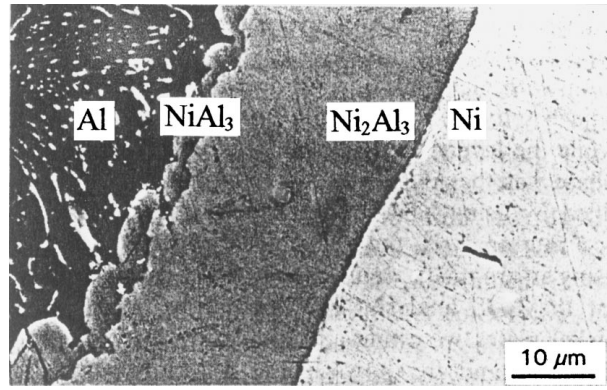

Figure 6 Microstructure of the interface in the Al/Ni diffusion couple annealed at 750°C for 25 minutes [41].

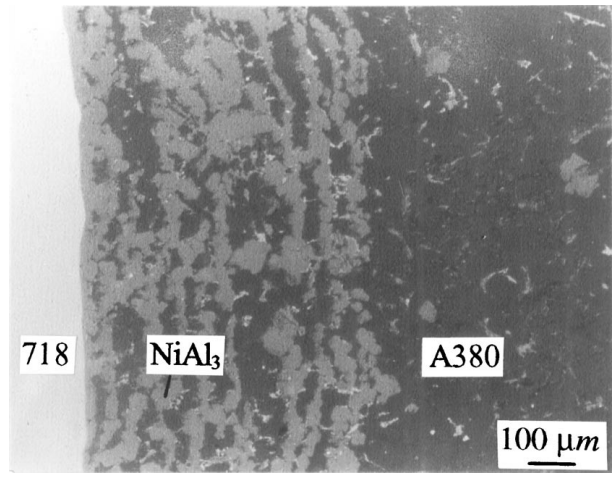

Figure 7 Morphology at the intermediate zone of Inconel 718/A380 alloy after 4 h test. Rotating at 700°C with a speed of 300 rpm [37].

TABLE III Erosion rates of some engineering materials rotating in semi-solid aluminum slurry at 600°C with a speed of 200 rpm [45]

Material	Erosion rate (μm/h)
Stellite 6B	200
Stellite 12	170
Alloy 718	450
Alloy 909	300
Tool steels	>300
Ti-6Al-4V	2–20
Ti-6Al-2Sn-4Zr-2Mo	12–45

2.3. Titanium-base alloys

Titanium is very corrosion resistant in molten aluminum, compared with steels and nickel-base alloys [23, 45]. The erosion rates of Ti alloys were most systematically investigated by Mihelich *et al*. [45], as listed in Tables III and IV. In the erosion test material was stirred as a blade of a stirrer agitating in Al-alloy slurry at 600°C with a stirring speed of 200 rpm (Table III), or at 625°C with a stirring speed of 205 rpm for a period of 11 hours (Table IV). Among all the investigated metals Ti alloys have the lowest erosion rates except the Nb-30Ti-20W alloy.

Titanium is least soluble in liquid aluminum among elements listed in Table II. The low solubility makes

TABLE IV Erosion rates of Ti- or Nb-base alloys rotating in A356/601 alloy at 625°C with a speed of 205 rpm for 11 hours [45]

Material	Erosion rate (μm/h)
Ti-6Al-4V (cast)	23
Ti-6Al-4V (cast) tiodised	20
Ti-6Al-4V (extruded)	25
Ti-6Al-4V (extruded) tiodised	24
Ti-6Al-2Sn-4Zr-2Mo (cast)	28
Ti-6Al-2Sn-4Zr-2Mo (cast) tiodised	24
Ti-0.2Pd (extruded)	14
Ti-0.2Pd (extruded) tiodised	16
Nb-30Ti-20W nitrided	6
Nb-30Ti-20W carbo-nitrided	6

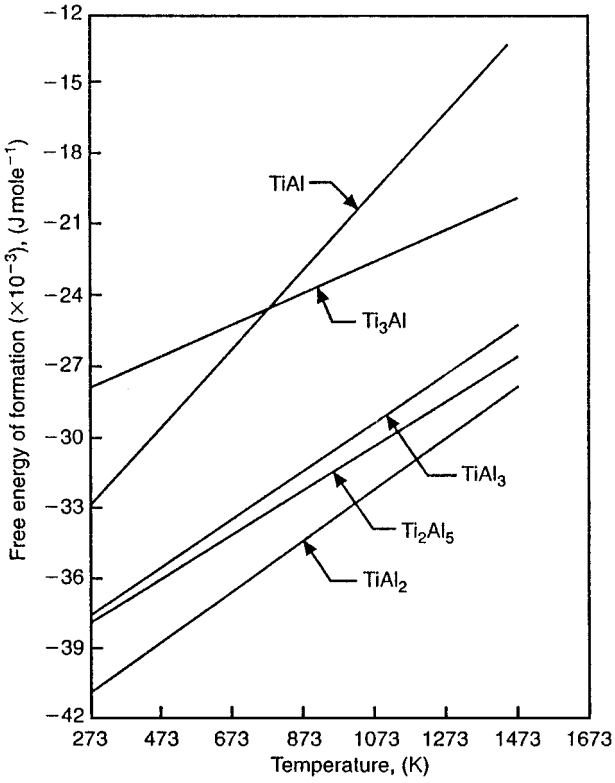

Figure 8 Free energies of formation of different Ti-Al compounds as a function of temperature [46].

the liquid layer surrounding the solid titanium more readily saturated with titanium solute. The saturation inhibits the further dissolution of titanium. Moreover, the high hardness of titanium makes it advantageous in the erosion environment. Although many intermetallic compounds exist in the binary Ti-Al phase diagram, it has been found that the formation of $TiAl_3$ between solid titanium and liquid aluminum is essential during many related processes, and only Ti_3Al, TiAl, and $TiAl_3$ can form by reactions involving solid titanium and solid aluminum [46]. Based on a thermodynamic assessment, Sujata *et al*. [46] found that $TiAl_3$ has the minimum free energy of formation among the compounds Ti_3Al, TiAl, and $TiAl_3$ at temperatures up to 1200°C (Fig. 8). Thus, the intermediate compound formed between solid titanium and pure liquid/solid aluminum below 1200°C is $TiAl_3$. Small additions of alloying elements don't change the crystal structure of $TiAl_3$, but beyond some limits new compounds may form. For Ti-Ti joints brazed with Al-Si filler alloys at 600°C for 3 min, only $TiAl_3$ forms in alloys containing up to 0.8 wt%Si, but in alloy containing 3 wt%Si, Ti_9Al_{23} and $Ti_7Al_5Si_{12}$ also form [18].

The low solubility suppresses the growth of the intermediate layer at the interface of solid titanium and molten aluminum. The layer is found to be planar and rather thin. Only about 3 μm thick layer is observed at the solid titanium-liquid aluminum interface while under the same conditions the intermediate zone of stainless steel is about 30 μm thick [23]. The thicknesses of intermediate layers of Ti-alloys investigated in Tables III and IV are reported to be 30 to 60 μm [45]. The growth of the intermediate layer between solid titanium and pure molten aluminum is controlled by the diffusion rate. Additions of alloying elements, such as Si, Mg, Ge, Cu, Li, Sb, Fe, Mn, Ti, Zr, and Ni, into liquid aluminum suppress the growth of intermediate layer. Among them silicon is the most effective element while nickel has the least effect [18].

2.4. Other alloys

Other metallic alloys investigated in terms of corrosion or dissolution in molten aluminum include Cr, Mo, Nb and Y, etc. In the Al-Cr system, β, γ and δ are three sorts of compounds present at the aluminum side of binary Al-Cr phase diagram. They have not certain composition formula, and contain chromium around 21 wt%, 26 wt% and 32 wt% respectively. In Barbier *et al*.'s work [21] the δ and β phases are found to form at 800°C at the Al-Cr interface, and there is another intermetallic layer with unknown composition between these two phases. In Tunca *et al*.'s work [47] the intermetallic phases formed at Al-Cr interface are found to be δ, γ and β at 735 and 785°C, listed in sequence from the chromium side to the aluminum side, while at 835 and 885°C only δ and β phases are observed.

At Al-Mo interfaces, Mo_3Al_8, Mo_4Al_{17}, Mo_5Al_{22}, and $MoAl_5$ are found to form at 735 and 785°C, while at 835°C only Mo_3Al_8, Mo_4Al_{17} and Mo_5Al_{22} are present, and Mo_3Al_8, $MoAl_4$, Mo_4Al_{17} at 915°C. In the temperature range from 735 to 885°C, only one intermetallic phase, $NbAl_3$, forms at the Al-Nb interface. At the Al-Y interface, a Y-containing intermetallic phase is also observed [47]. The solubility of solid Cr, Mo, and Nb in liquid aluminum is presented in Fig. 9 as the function of temperature. It can be seen that in Al-Cr and Al-Mo systems there is not any slope change in C_s-1/T curves, although different intermetallic phases are in equilibrium with molten aluminum at different temperatures. The solubility of niobium in aluminum is much lower than that of Cr and Mo. The low values for niobium in Fig. 9 confirm the relevant data in Ref. [48], although lower than in Ref. [49]. For the Al-Y system, the solubility of yttrium in molten aluminum is found to be drastically affected by impurities in yttrium matrix and the occurrence of intermetallic phase at the Al-Y interface [47].

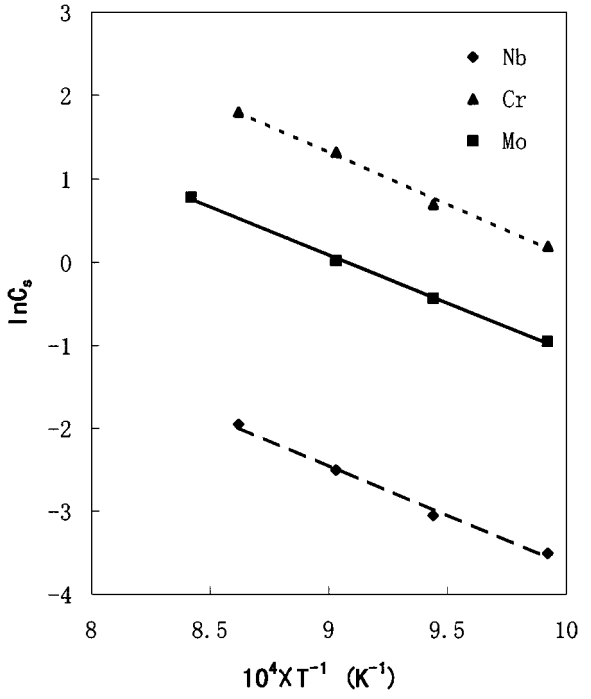

Figure 9 The solubility of solid chromium, molybdenum, and niobium in liquid aluminum, C_s, as the function of temperature, T [47].

A Nb-base alloy (Nb-30Ti-20W) is selected for fabrication of components like barrel and screw in a patented equipment for semi-solid Al-alloy processing [45]. This alloy is found to be the best and superior to Ti-alloys in resisting erosion by molten aluminum (Table IV). The substantially reduced erosion rate is connected with the low solubility of niobium in molten aluminum, and the high bulk hardness of the alloy (HV600).

3. Ceramics

Ceramics investigated in the search for materials chemically compatible with molten aluminum are generally industrially available, including graphite, aluminosilicate refractories, AlN, Si_3N_4, SiC, Al_2O_3, and sialons. Among them, some have been characterized satisfactory for specific applications with molten aluminum.

The corrosion resistance and mechanical properties of ceramics are affected by the chemical compositions and processing conditions, such as firing temperature, pressing pressure. To avoid infiltration by aluminum, the ceramic should be free of porosity and any constituent component which is prone to dissolve in molten aluminum. It is noteworthy that the reactivity of ceramics with molten metals other than aluminum can not be used as indicators of their chemical reactivity with molten aluminum due to different phase relationships. For example, Si_3N_4 is found to be prone to degradation in ferrous alloy [50], but as will be discussed later, it is quite inert in aluminum.

3.1. Ceramics characterized inert in molten aluminum

So far, ceramics which have been characterized chemically inert in liquid aluminum include graphite, aluminosilicate refractories, AlN, Si_3N_4, Al_2O_3, and sialons. They will be discussed in the following subsections.

3.1.1. Graphite

There have been many investigations on the reaction of molten aluminum and carbon systems, with the objective of promoting wetting of aluminum on carbon fibres without serious attack of the fibres or formation of an intermediate compound during fabrication of carbon fiber-reinforced aluminum composites [12, 51]. The carbide Al_4C_3 is the only intermediate compound reported in the system [51] through the following reaction:

$$4Al + 3C = Al_4C_3 \quad (1)$$

Al_4C_3 is thermodynamically favored at temperatures above the melting point of aluminum. *In situ* sessile drop experiments of liquid aluminum on carbon substrates revealed that a thick film of aluminum carbide is formed at temperatures above 1000°C [12], and decomposed to carbon-saturated melt and graphite at approximately 2150°C [52]. The reactivity between Al and C is weak at temperatures below 1000°C, partly due to the presence of an oxide layer [12]. In the literature measurements on the solubility of carbon in molten aluminum at lower temperatures have a significant discrepancy, although fairly consistent in the temperature range of 1600–2600°C [51–53]. The result of Al_4C_3 solubility in molten aluminum in the temperature range of 950–1000°C calculated by Qiu *et al*. are in agreement with the experimental data obtained by Simenmen (Fig. 10) [51]. Through extrapolating the curve to the lower temperature range below 700°C, which normally applies in semi-solid processing of aluminum, the solubility of Al_4C_3 is extremely low.

As one of the most cost-efficient material, graphite has been well-known for its compatibility with aluminum melt and the ease of fabrication. However, its brittleness makes it impossible for the fabrication of components where stress-bearing is a requirement.

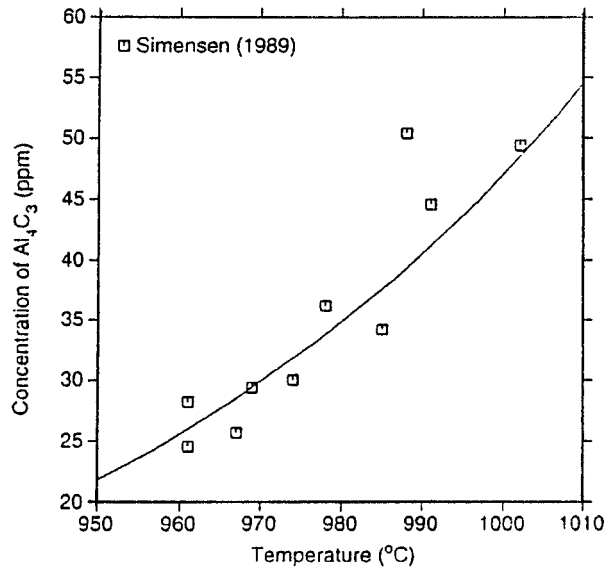

Figure 10 Comparison between the calculated and experimental carbide solubility in liquid aluminum [51].

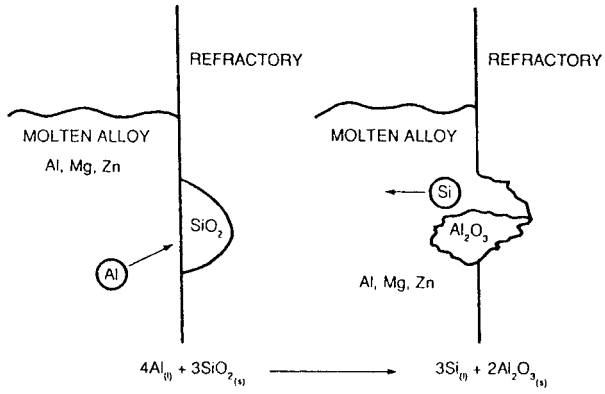

Figure 11 Schematic diagram showing the mechanisms of molten aluminum alloy attack on a silica-containing refractory. Alloy is lost by penetration and reaction with the refractory while silicon is released into the alloy [55].

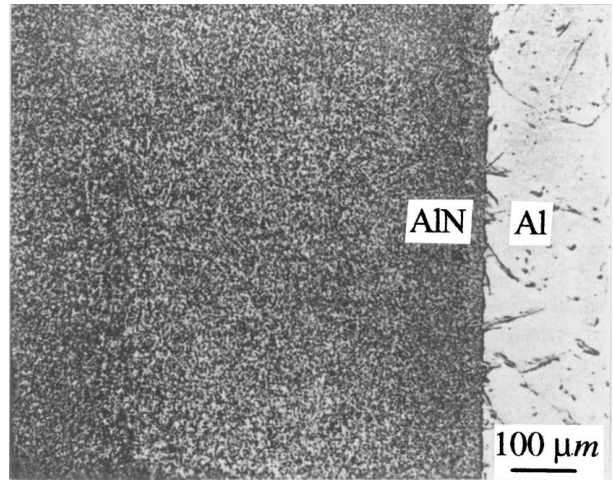

Figure 12 Interface of AlN and high purity aluminum after heating to 2000°C in carbon monoxide atmosphere [59].

3.1.2. Aluminosilicate refractories

Aluminosilicate refractories are well-known for their applications in melting and holding furnaces. Considerable effort has been carried out to develop new materials compatible with molten aluminum. The protection mechanisms, however, are complex and not yet well understood. It is generally believed that molten aluminum alloys attack aluminosilicate refractories by redox reactions in which silica and silicates in the refractory are reduced to form elemental silicon while metallic aluminum forms aluminum oxide [54–57]. The rate of attack is known to be proportional to the silica content in the refractory, and especially that of the matrix phase [54]. The mechanism of attack depends on the transport of elemental species and also on the redox reaction. While aluminum and alloying elements diffuse into the refractory, silicon is released by the redox reaction and counterdiffuses into the molten alloy (Fig. 11). As a result, a reaction layer containing alumina is present after an incubation period, and acts as a barrier against further melt penetration.

Many non-wetting agents, such as CaF_2, AlF_3, and $BaSO_4$, have been used to improve the corrosion resistance of refractories [58]. However, in the presence of alkalis and under a reducing atmosphere the extent of corrosion increases [57]. This is because alumina transforms to sodium aluminate, and the transformation kinetics are enhanced. Lower silica content or addition of dopants, such as rare earths, improves resistance to liquid aluminum alloys [55]. But alloying elements such as magnesium and zinc in aluminum alloys can undermine the protective effect of alumina, making corrosion occur in a continuous manner. Therefore, to choose the most appropriate refractory requires knowledge of alloy type, furnace type and in-service conditions.

3.1.3. AlN

As a high temperature structural ceramic and hard refractory material, AlN is a candidate refractory container for molten metals [59, 60]. It possesses an intrinsic inertness, and a high hardness [61]. Long *et al*. [59] report that in both argon and CO atmospheres AlN has an unnoticeable attack by molten aluminum at a temperature as high as 2000°C, and in oxidizing atmosphere like wet and dry air, only above 1200°C does appreciable attack occur to AlN. A section of AlN crucible containing aluminum after heating to 2000°C is demonstrated in Fig. 12. The needles in the figure are Al_4C_3, coming from reaction of the CO atmosphere with aluminum and being not the product of AlN-Al reaction. However, during the processing of AlN/Al composite the infiltration of AlN by aluminum in vacuum at 1220–1280°C is found to occur with a relatively high activation energy, suggesting a chemical interaction between AlN and aluminum [62]. It reveals that the inertness of AlN in molten aluminum may need some conditions, and a reducing atmosphere is favorable.

3.1.4. Al_2O_3

Al_2O_3 is one of the most widely applied crucible materials. It is not wetted by molten aluminum below 1000°C, and considered to be inert in molten iron and nickel [50]. Although some investigations on the wettability of Al_2O_3 with molten aluminum indicate that Al_2O_3 may be attacked by molten aluminum [63], there has been no data on its corrosion rate. Both Al-Li and Al-Mg alloys reacted with pure alumina in argon atmosphere. In Al-Mg alloys it forms stable $MgAl_2O_4$ spinel [43]. SIMS revealed that 0.02–0.13 nm thick $LiAlO_2$ and $MgAl_2O_4$ formed respectively at the interfaces of Al_2O_3 with Al-Li and Al-Mg alloys at 700°C [64]. The thickness of the $LiAlO_2$ layer increases proportionally to the increase of lithium content in Al-Li alloys, the reaction temperature, and the square root of time.

3.1.5. Si_3N_4 and sialons

Si_3N_4 has been considered to be corrosion resistant in aluminum. The formation of a dense protective intermediate AlN layer at the interface is found to be responsible for the high durability of Si_3N_4 in molten aluminum [13, 65–68]. Addition of 30 wt% Si_3N_4 to a MgO-CaO-Al_2O_3-SiO_2-TiO_2 glass ceramic enables it to withstand molten aluminum at 800°C for 400 h without visible corrosion, while the same material without

Si_3N_4 is highly corroded after only 0.5 hour under the same conditions [69].

Sialons are generally synthesized through sintering at high temperatures above 1600°C in nitrogen atmosphere. The main raw materials are Si_3N_4 and Al_2O_3. Al_2O_3 is an intermediate glass former capable of forming a network with silica and other network formers. This binding phase surrounding Si_3N_4 grains can be either glassy silicate or crystalline phases, or a mixture of both, depending on the composition and the cooling rate. The special network makes the sialon matrix more difficult to disrupt physically and more chemically stable, and this has been proved in our laboratory.

3.2. Ceramic materials active in molten aluminum

3.2.1. SiC

In molten aluminum SiC is active and corrodes at a high rate. SiC can react with molten aluminum, producing Al_4C_3 and silicon, according to the following reaction [70]

$$4Al + 3SiC = Al_4C_3 + 3Si \quad (2)$$

Silicon produced through the above reaction dissolves in aluminum, giving rise to an Al-Si alloy [71, 72]. Viala *et al*. systematically investigated the chemical interaction of SiC with molten aluminum [70, 72]. It is found that from 657 to 827°C, α-SiC interacts with aluminum via a dissolution-precipitation process. This mechanism involves the migration of carbon atoms from places where the SiC surface is in direct contact with the aluminum to the growing faces of Al_4C_3 crystals located at or close to the aluminum-SiC interface. The decomposition rate greatly depends on the polarity of the SiC surface exposed to aluminum. Lateral extension of Al_4C_3 on the (0001) Si face of a SiC single crystal and randomly oriented faces results in the formation of an adherent, dense and continuous layer of Al_4C_3, which can protect the underlying substrate from further attack. However, passivation from Al_4C_3 never occurs on the (0001)C face of the SiC crystal because Al_4C_3 can not nucleate and bond onto the face. Thus the C face is damaged more heavily than other faces. Fig. 13 shows the variation of average decomposition depths at Si and C faces of SiC in aluminum at 727°C with the reaction time.

It is found that the interaction between SiC and aluminum alloy intensifies when introducing 3–7% silicon into aluminum [73].

3.2.2. B_4C

B_4C has a high hardness just below that of diamond, excellent thermal stability, and is considered to have significant chemical inertness. However, it has been observed that B_4C can react not only with liquid aluminum, but even with solid aluminum [15]. Carbon and boron atoms can diffuse into liquid aluminum from the surface of B_4C. In the temperature range of 660°C (melting point of aluminum) to 868°C, the reaction products of Al-B_4C mixture are Al_3BC and AlB_2, which are the same as those observed through reaction of solid B_4C and solid aluminum. Above 868 ± 4°C AlB_2 is replaced by $Al_3B_{48}C_2$ while Al_3BC remains stable. A continuous layer of Al_3BC, once formed, may constitute an efficient diffusion barrier and provide protection for B_4C.

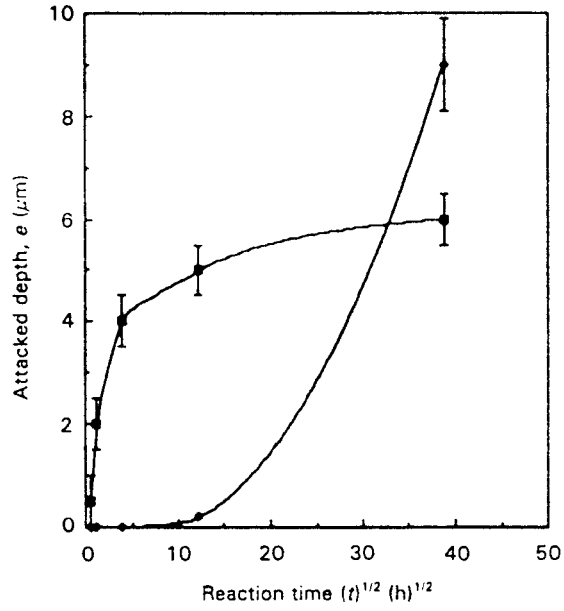

Figure 13 Variation of the average decomposition depth, *e*, of SiC single crystals in liquid aluminum at 727°C with the reaction time, *t*: (■) Si face, and (●) C face [70].

3.2.3. TiC_x and Cr_2O_3

Titanium carbide has been characterized as not inert with aluminum, through investigations on the phase equilibrium and transformation occurring in the ternary system Al-C-Ti, as well as reaction of TiC particles with liquid aluminum. Al_4C_3 and Ti_xAlC are found to form at the interface of TiC particles and liquid aluminum [74]. In Viala *et al*.'s work, a quisi-peritectic reaction occurs at 812 ± 15°C between TiC_x ($x < 0.9$) and liquid aluminum [75]:

$$Al + TiC_x \rightarrow Al_3Ti + Al_4C_3 \quad (3)$$

Through the reaction TiC_x is decomposed by aluminum.

Cr_2O_3 is observed to be attacked by aluminum alloys at temperatures even below 750°C. The loss rate curve of a 50 μm thick Cr_2O_3 coating on a H21 steel bar rotating in molten A380 alloy, which is obtained in our laboratory, is given in Fig. 14 against the square root of test time. The diameter of the steel bar is 10 mm, and the test temperature is 700°C. Further research on the attack mechanisms of Cr_2O_3 has not been conducted so far.

4. Discussion

According to the research results, to warrant satisfactory performance in molten aluminum the materials

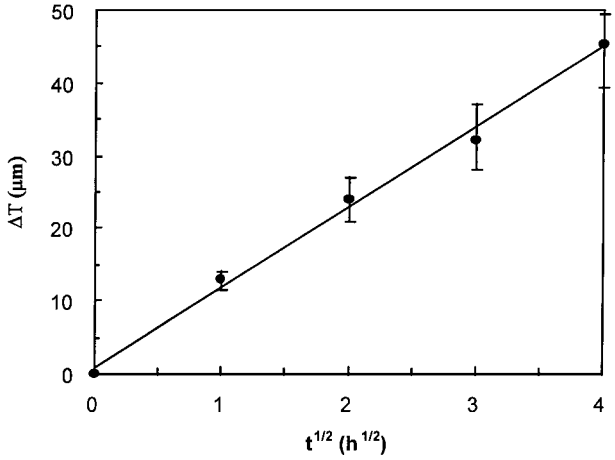

Figure 14 The average thickness loss of Cr_2O_3 coating on H21, ΔT, vs. the square root of test time. Sample diameter 10 mm, rotating in molten A380 alloy at 700°C with a speed of 300 rpm.

should possess the following characteristics, in addition to necessary mechanical and thermal properties:

(1) Low solubility in liquid aluminum. Solubility is deemed as a factor of the most importance for the corrosion rate.

(2) Limited thickness and dissolution rate of the interfacial layer in aluminum.

(3) The interfacial layer should be dense to act as a diffusion barrier, and well bonded to the substrate.

(4) A high hardness intermetallic layer is required to provide protection against wear and erosion under dynamic conditions.

4.1. Establishment of the interfacial layers

In both ceramics and metal alloys, atoms of the solid materials dissolve and diffuse into the melt or the intermediate zone in the initial stage of interaction. This occurs on a small scale, generally as individual atoms. At this stage the corrosion rate is controlled by the interfacial reaction, and is theoretically linear with the reaction time. The next stage involves the diffusion of elements from substrate and aluminum melt in the intermetallic layers, dissolution of the layers and sometimes, the release of material from the interfacial layers which proceeds in blocks. At this stage the interfacial layer is established and grows thicker with the reaction time. The corrosion rate is now diffusion controlled, and proportional to the square root of time, following the parabolic law. The corrosion depth, T, is generally expressed depending on the following equation [76, 77]

$$T = Ct^n \tag{4}$$

Where C is a constant, n equals 1 at the beginning of the reaction and finally reaches 0.5. However, the practically measured data of n often deviate from these standard values and vary when the reaction proceeds.

Once formed, the intermediate layer itself is critical to the reaction rate. When a stable, compact, and well-bonded intermetallic layer forms passivation occurs on the solid surface, for example, in the cases of Si_3N_4 and titanium. A thick layer, however, does not necessarily inhibit the corrosion effectively. On the contrary, materials possessing high solubility in liquid aluminum, such as nickel, which forms thick layers of intermetallic compounds, is prone to corrosion. Materials with high corrosion resistance only form thin layers. For inert ceramics the formation of interfacial compounds needs incubation, or even is not possible below certain temperatures.

4.2. Effect of dynamic agitation

It is well established that the dissolution of a solid metal in a liquid metal can be described by the following equation [30, 78]

$$\ln\left(\frac{c_s - c_0}{c_s - c}\right) = k\frac{St}{V} \tag{5}$$

Where c is the concentration of the solute element in the melt, c_s the saturation concentration, c_0 the initial concentration of the solute, k the dissolution rate constant, S the solid metal surface, V the melt volume, and t time. For a fixed volume of melt, when the dissolution proceeds the concentrations of dissolved elements rise, resulting in decreasing in the rate of further dissolution.

When stirring is present in the melt, the dissolution rate constant, k, can be calculated by the equations below [20, 30, 79]

$$k = 0.62D^{2/3}\nu^{-1/6}\omega^{1/2} \quad \left(Sc = \frac{\nu}{D} > 1000\right) \tag{6}$$

and

$$k = 0.554I^{-1}D^{2/3}\nu^{-1/6}\omega^{1/2} \quad (4 < Sc \leq 1000) \tag{7}$$

Here ω is the angular rotating speed of the solid metal, ν the kinematic viscosity of melt, D the diffusion coefficient of solute across the interfacial zone and $I = \mathrm{f}(Sc)$.

From the above equations it can be seen that the presence and intensity of agitation affect the dissolution rate of solids in liquid. Another important loss mechanism from agitation is that agitation may damage the protective layer or accelerate the wear by the detachment of the reaction product, such as protuberances. The effect of melt agitation is much more drastic for those materials which form thick reaction layers which do not adhere well to substrate and are not hard enough.

4.3. Effect of surface coatings

An important approach to surface protection in molten aluminum is surface coating. Significant improvement of protection effect through coating has been achieved [80]. When a coating is used for materials protection the coating efficiency depends strongly on its adhesion to the substrate, and the chemical inertness of the coating materials. For protection in wear and corrosion conditions, the hardness and toughness of the coating are also important. Ceramics are generally selected as the coating materials. The main concern for ceramic coatings is whether the coating itself could survive for a satisfactory service life, especially under dynamic conditions, since under such circumstances erosion from

the liquid aluminum leads to the cracking and loss of coatings.

4.4. Effect of the grain size

Reports on the effect of grain size on materials durability in molten aluminum are limited. For ceramics of high corrosion resistance, the boundary layers, if forming, need the time of inoculation. In such cases, grain size may affect the corrosion rate. Grain boundaries may be a shortcut for elemental diffusion, and greater surface area may speed up the corrosion rate. In liquid iron-, nickel-base alloys penetration by liquid metal along grain boundaries into the ceramic causes wear, and make the ceramic adjacent the penetrated grain boundaries to dissolve into the liquid metal [50]. Exposure of TiB_2 in molten aluminum has been found to lead to embrittlement of the material, due to intergranular penetration of aluminum as well as impurity elements [81, 82].

5. Summary

Ceramics such as graphite, aluminosilicate refractories, AlN, Al_2O_3, Si_3N_4, and sialons are characterized as inert in molten aluminum and its alloys, among them, AlN, Si_3N_4 and sialons can be considered for application under complex stress conditions due to their favorable mechanical properties. The chemical compositions and processing conditions have significant effects on their corrosion resistance and mechanical properties. Infiltration by aluminum has to be avoided. Therefore, ceramic should be free of any element in the interconnected phases prone to dissolve in molten aluminum, and be free of porosity.

The corrosion resistance of metals is generally poorer than that of inert ceramics. Good fabricability, toughness and cheapness, however, are their advantages. Solubility in liquid aluminum is the most important factor for the durability of alloys. Since reaction layers are generally present at the metal-aluminum interface, the presence and the intensity of melt agitation plays an important role in erosion of solid metals in liquid aluminum. Among the commonly used engineering metals the durability of titanium and niobium are very good. Moreover, the lifetime of metals, such as steels, in molten aluminum can be greatly prolonged through application of suitable ceramic coatings according to in-service conditions.

References

1. R. E. PARDEE, *J. Inst. Met.* **94** (1966) 56.
2. A. G. FURNESS and C. F. PYGALL, *Trans. J. Br. Ceram. Soc.* **82** (1983) 213.
3. S. AFSHAR and C. ALLAIRE, *J. Minerals Met. Mater. Soc.* **48** (1996) 23.
4. M. YU, R. SHIVPURI and R. RAPP, *J. Mater. Eng. Performance* **4**(2) (1995) 175.
5. M. SUNDQVIST and S. HOGMARK, *Tribology Inter.* **26** (1993) 129.
6. D. H. KIRKWOOD, *Inter. Mater. Rev.* **39** (1994) 173.
7. R. F. DECKER, R. D. CARNAHAN, R. VINING and E. ELDENER, in 4th Inter. Conf. on Semi-Solid Processing of Alloys and Composites, edited by D. H. Kirkwood and P. Kapranos (University of Sheffield, UK, 1996).
8. W. E. LEE and Z. SHANG, *Int. Mater. Review* **44** (1999) 1.
9. N. SOBCZAK, Z. GORNY, M. KSIAZEK, W. RADZIWILL and P. ROHATGI, *Mater. Sci. Forum* **217** (1996) 153.
10. D. A. WEIRAUCH, W. M. BALABA and A. J. PERROTTA, *J. Mater. Res.* **10** (1995) 640.
11. P. D. OWNBY, K. W. LI and D. A. WEIRAUCH, JR., *J. Amer. Ceram. Soc.* **74** (1991) 1275.
12. N. EUSTATHOPOULOS, J. C. JOUD, P. DESRE and M. HICTER, *J. Mater. Sci.* **9** (1974) 1233.
13. L. MOURADOFF, A. LACHAU-DURAND, J. DESMAISON and J. C. LABBE, *J. European Ceramic Soc.* **13** (1994) 323.
14. S. D. PETEVES, *Ceram. Inter.* **22** (1996) 527.
15. J. C. VIALA, J. BOUIX, G. GONZALEZ and C. ESNOUF, *J. Mater. Sci.* **32** (1997) 4559.
16. J. P. TU and M. MATSUMURA, *Scripta Metall.* **40** (1999) 645.
17. J. P. TU, J. PAN, M. MATSUMURA and H. FUKUNAGA, *Wear* **223** (1998) 22.
18. T. TAKEMOTO and I. OKAMOTO, *J. Mater. Sci.* **23** (1988) 1301.
19. N. KOMATSU, M. NAKAMURA and H. FUJITA, *J. Inst. Light Metals* **18** (1968) 474.
20. V. N. YEREMENKO, YA. V. NATANZON and V. I. DYBKOV, *J. Mater. Sci.* **16** (1981) 1748.
21. F. BARBIER, D. MANUELLI and K. BOUCHE, *Scripta Mater.* **36** (1997) 425.
22. G. EGGELER, W. AUER and H. KAESCHE, *J. Mater. Sci.* **21** (1986) 3348.
23. A. W. BATCHELOR, N. P. HUNG and T. K. LEE, *Tribology Inter.* **29** (1996) 41.
24. TH. HEUMANN and S. DITTRICH, *Z. Metallkde* **50** (1959) 617.
25. PH. VAILLANT and J. P. PETITET, *J. Mater. Sci.* **30** (1995) 4659.
26. M. NIINOMI and Y. UEDA, *Trans. Jap. Inst. Met.* **23** (1982) 709.
27. M. YAN and Z. FAN, *J. Mater. Sci.* **35** (2000) 1661.
28. K. BOUCHE, thesis, University of Provence, Marseille, France, 1995.
29. S. G. DENNER, R. D. JONES and R. J. THOMAS, *Iron and Steel Inter.* (1975) June, 241.
30. V. I. DYBKOV, *J. Mater. Sci.* **25** (1990) 3615.
31. J. E. NICHOLLS, *Corr. Technol.* **11** (1964) 16.
32. H. BERNS, in Proc. Inter. Conf. on Tool Materials for Molds and Dies, Illinois, 1987, p. 45.
33. B. GIEREK, *Bulletin Swedish Corrosion Institute* **77** (1977) 1.
34. T. HEUMANN and S. DITTRICH, *Z. Metallkde.* **50** (1959) 617.
35. D.I. LAINER and A. K. KURAKIN, *Fiz. Met. Metallov.* **18** (1964) 145.
36. C. COLIN, thesis E.N.S.M.P., Paris, 1994.
37. M. YAN, Z. FAN and M. J. BEVIS, *Scripta Metall.* **40** (1999) 1255.
38. M. M. P. JANSSEN and G. D. RIECK, *Trans. TMS-AIME* **239** (1967) 1372.
39. L. S. CASTLEMEN and L. L. SEIGLE, *ibid.* **209** (1957) 1173.
40. *Idem.*, *ibid.* **212** (1958) 589.
41. C. L. TSAO, S. W. CHEN, *J. Mater. Sci.* **30** (1995) 5215.
42. F. DELANNAY, L. FROYEN and A. DERUYTTERE, *ibid.* **22** (1987) 1.
43. D. A. WEIRAUCH, JR, *ibid.* **3** (1988) 729.
44. "Metals Handbook Vol. 8: Metallography, Structures and Phase Diagrams," 8th ed. (ASM, USA, 1973).
45. J. MIHELICH and R. F. DECKER, US Patent no. 5711366, (1998).
46. M. SUJATA, S. BHARGAVA and S. SANGAL, *J. Mater. Sci. Lett.* **16** (1997) 1175.
47. N. TUNCA, C. W. DELAMORE and R. W. SMITH, *Met. Trans. A* **21** (1990) 2919.
48. V. N. YEREMENKO, YA. V. NATANZON and V. I. DYBKOV, *J. Less-Common Met.* **50** (1976) 29.
49. M. A. WICKER, C. ALLIBERT and J. DRIOLE, *C.R. Acad. Sci. Ser. C* **272** (1971) 1711.
50. J. A. YEOMANS and T. F. PAGE, *J. Mater. Sci.* **25** (1990) 2312.

51. C. QIU and R. METSELAAR, *J. Alloys Compounds* **216** (1994) 55.
52. L. L. OLDEN and R. A. MCCUNE, *Met. Trans. A* **18** (1987) 2005.
53. C. J. SIMENSEN, *ibid*. **20** (1989) 191.
54. K. J. BLONDYKE, *J. Amer. Ceram. Soc*. **36** (1953) 171.
55. M. H. O'BRIEN and M. AKINC, *ibid*. **72** (1989) 896.
56. H. MIYAHARA, J. OTANI, N. MORI and K. OGI, *J. Japan Inst. Met*. **56** (1992) 1056 (in Japanese).
57. C. ALLAIRE and P. DESCLAUX, *J. Amer. Ceram. Soc*. **74** (1991) 2781.
58. T. H. HALL and G. WILSON, in Proc. Inter. Symp. Advances in Refractories (Pergamon Press, 1988) p. 225.
59. G. LONG and L. M. FOSTER, *J. Amer. Ceram. Soc*. **42** (1959) 53.
60. C. TOY and W. D. SCOTT, *J. Mater. Sci*. **32** (1997) 3243.
61. N. ICHINOSE, "Introduction to Fine Ceramics, Applicatuions in Engineering" (English translation) (Wiley, New York, 1987) p. 49.
62. C. TOY and W. D. SCOTT, *J. Amer. Ceram. Soc*. **73** (1990) 97.
63. V. LAURENT, D. CHATAIN, C. CHATILLION and N. EUSTHAPOULOS, *Acta Metall*. **36** (1988) 1797.
64. H. MIYAHARA, R. MURAOKA, N. MORI and K. OGI, *J. Japan Inst. Met*. **59** (1995) 660 (in Japanese).
65. L. MOURADOFF, *Key Eng. Mater*. **113** (1996) 177.
66. W. X. PAN, T. OKAMOTO and X. S. NING, *J. Mater. Sci*. **29** (1994) 1436.
67. X. S. NING, T. OKAMOTO and Y. MIYAMOTO, A. KOREEDA, K. SUGANUMA, *ibid*. **26** (1991) 4142.
68. I .RIVOLLET, D. CHATAIN and N. EUSTATHOPOULOS, *ibid*. **25** (1990) 3179.
69. I. PENKOV, R. PASCOVA and I. DRANGAJOVA, *J. Mater. Sci. Lett*. **16** (1997) 1544.
70. J. C. VIALA, F. BOSSELET, V. LAURENT and Y. LEPETITCORPS, *J. Mater. Sci*. **28** (1993) 5301.
71. V. M. BERMUDEZ, *Appl. Phys. Lett*. **42** (1983) 70.
72. J. C. VIALA, P. FORTIER and J. BOUIX, *J. Mater. Sci*. **25** (1990) 1842.
73. A. A. AKSENOV, E. A. CHURMUKOV, V. S. ZOLOTOREVSKII and G. V. INDENBAUM, *Russian Metall*. **1** (1995) 19 (in Russian).
74. P. S. MOHANTY, J. E. GRUZLESKI, *Scripta Metall. Mater*. **31** (1994) 179.
75. J. C. VIALA, C. VINCENT, H. VINCENT and J. BOUIX, *Mater. Res. Bull*. **25** (1990) 457.
76. C. F. OLD and I. MACPHAIL, *J. Mater. Sci*. **4** (1969) 202.
77. S. K. KANG and V. RAMACHANDRAN, *Scripta Metall*. **14** (1980) 421.
78. L. L. BIRCUMSHAW and A. C. RIDDIFORD, *Quart. Rev*. **6** (1952) 157.
79. T. F. KASSNER, *J. Electrochem. Soc*. **114** (1967) 689.
80. A. WYNN, *Br. Ceram. Trans. J*. **91** (1992) 153.
81. H. R. BAUMGARTNER, *J. Amer. Ceram. Soc*. **67** (1984) 490.
82. C. B. FINCH and V. J. TENNERY, *ibid*. **65** (1982) 100.

Received 19 May 1999
and accepted 5 April 2000